MAJOR ARTICLE

# Early Systemic Bacterial Dissemination and a Rapid Innate Immune Response Characterize Genetic Resistance to Plague of SEG Mice

**Christian E. Demeure,[1] Charlène Blanchet,[2,a] Catherine Fitting,[3] Corinne Fayolle,[1,a] Huot Khun,[4] Marek Szatanik,[2,a] Geneviève Milon,[5] Jean-Jacques Panthier,[2] Jean Jaubert,[2] Xavier Montagutelli,[2] Michel Huerre,[4] Jean-Marc Cavaillon,[3] and Elisabeth Carniel[1]**

[1] *Yersinia* Research Unit, [2]Mouse Functional Genetics Unit, [3]Unité Cytokines et Inflammation, [4]Unité de Recherche et d'Expertise Histotechnologie et Pathologie, and [5]Unité Immunophysiologie et Parasitisme Intracellulaire, Institut Pasteur, Paris, France

***Background.*** Although laboratory mice are usually highly susceptible to *Yersinia pestis*, we recently identified a mouse strain (SEG) that exhibited an exceptional capacity to resist bubonic plague and used it to identify immune mechanisms associated with resistance.

***Methods.*** The kinetics of infection, circulating blood cells, granulopoiesis, lesions, and cellular populations in the spleen, and cytokine production in various tissues were compared in SEG and susceptible C57BL/6J mice after subcutaneous infection with the virulent *Y. pestis* CO92.

***Results.*** Bacterial invasion occurred early (day 2) but was transient in SEG/Pas mice, whereas in C57BL/6J mice it was delayed but continuous until death. The bacterial load in all organs significantly correlated with the production of 5 cytokines (granulocyte colony-stimulating factor, keratinocyte-derived chemokine (KC), macrophage cationic peptide-1 (MCP-1), interleukin 1α, and interleukin 6) involved in monocyte and neutrophil recruitment. Indeed, higher proportions of these 2 cell types in blood and massive recruitment of $F4/80^{+}CD11b^{-}$ macrophages in the spleen were observed in SEG/Pas mice at an early time point (day 2). Later times after infection (day 4) were characterized in C57BL/6J mice by destructive lesions of the spleen and impaired granulopoiesis.

***Conclusion.*** A fast and efficient *Y. pestis* dissemination in SEG mice may be critical for the triggering of an early and effective innate immune response necessary for surviving plague.

Plague has caused 3 pandemics that have killed 200 million human beings [1, 2]. Despite considerable progresses in its prevention and cure, the disease persists today on 3 continents (Africa, Asia, and Americas) [3] and has resurged in areas considered plague free for several decades, leading to its categorization as a reemerging disease [4]. This threat has been further exacerbated by the isolation of *Yersinia pestis* strains naturally resistant to antibiotics [5, 6] and by their potential use for bioterrorism.

Bubonic plague, the most common clinical presentation, results from the bite of infected fleas. After intradermal penetration, *Y. pestis* disseminates via lymphatic vessels to draining lymph nodes and then spreads to various tissues (spleen, liver) before causing a fatal septicemia [7, 8]. Without prompt diagnosis and antibiotherapy, bubonic plague is rapidly lethal in 50%–70% of cases [1]. Strikingly, little is known about the characteristics of the systemic and local host responses specifically targeted by *Y. pestis* during the infectious process.

During the Middle Ages, some individuals were able to survive bubonic plague, suggesting a genetic determinism of resistance. Nonhuman mammalian species display variable levels of susceptibility to plague [1]. The host

Received 8 March 2011; accepted 27 May 2011; electronically published 16 November 2011.

Presented in part: Ninth International Symposium on Yersinia, Lexington, Kentucky, 10–14 October 2006.

[a]Present affiliations: Unité Cytokines et Inflammation (C.B.), Service de l'Enseignement (C.F.), and Unité Postulante Infections Bactériennes Invasives (M.S.), Institut Pasteur, Paris, France.

Correspondence: C. E. Demeure, PhD, *Yersinia* Research Unit, Institut Pasteur, 28 rue du Dr Roux, Paris 75724, France (cdemeure@pasteur.fr).

**The Journal of Infectious Diseases 2011;205:134–43**



DOI: 10.1093/infdis/jir696

mechanisms responsible for these different responses are unknown but are most probably genetically determined. Even rodents, the major plague reservoir, display a wide susceptibility spectrum. The observation that the progeny of various rodent species trapped in plague foci are significantly more resistant to plague than their counterparts from nonplague foci [9–12] suggests the selection of protective allelic combinations under *Y. pestis* pressure.

Laboratory mice (*Mus musculus*), a widely used experimental model to study *Y. pestis* pathophysiology, are usually highly susceptible to plague (*Y. pestis* median lethal dose of ≈10 colony-forming units [CFU] on subcutaneous infection) [13]. However, mice resisting an intravenous inoculation of high doses of *Y. pestis* KIM5 were recently reported [14, 15]. Genetic studies subsequently showed that their resistance was at least in part associated with ≥30 cM of 129-derived genomic DNA near the *Il10* locus [16] or with the major histocompatibility complex region on chromosome 17 [15]. Some resistant strains (129 substrain) displayed an acute inflammatory cellular response [17] and others (BALB/cJ) a lower production of interleukin (IL) 6 [15]. Although these studies revealed valuable new information about genetic determinants and physiological mechanisms of resistance to plague, their drawback is that they used an attenuated *Y. pestis* KIM5 strain (deleted of the high-pathogenicity island) that had to be injected by a nonphysiological route (intravenous). The 129 mice were as susceptible as other laboratory mice when a fully virulent *Y. pestis* was injected subcutaneously [17].

We recently showed that the SEG/Pas (SEG) mouse strain exhibits high resistance to a SC infection with a fully virulent *Y. pestis* [18]. This mouse strain (*Mus spretus*) is derived from wild progenitors and has been established as an inbred strain [19]. Although 100 CFU killed 94% of the C57BL/6J (B6) animals, only 10% of SEG mice succumbed. Furthermore, the median lethal dose of *Y. pestis* for B6 was 3.2 CFU, whereas that for SEG was $>10^7$ CFU [18]. The availability of this mouse strain provided a unique opportunity to identify pathophysiological mechanisms of resistance to plague by comparing the infectious process and the host response in susceptible (B6) and resistant (SEG) animals.

## MATERIALS AND METHODS

### Bacterial Growth Conditions

*Yersinia pestis* CO92 was grown in Luria-Bertani (LB) broth or on LB agar supplemented with 0.2% hemin (LB-H) for 48 hours at 28°C in a level 3 biosafety (BSL3) laboratory. Kinetics of bacterial growth in mouse serum were determined by inoculating $10^3$ CFU/mL of CO92 grown at 37°C in undecomplemented pooled serum samples from 7 mice. The samples were incubated at 37°C for 48 hours, and aliquots were taken at various intervals, diluted, and plated on Luria Bertani-Hemin (LB-H).

### Mouse Experiments

Infection with *Y. pestis* was performed in a BSL3 animal facility according to the Institut Pasteur guidelines. Groups of female B6 (Charles River) or SEG (Institut Pasteur) mice aged 8–12 weeks received a subcutaneous injection of 100 CFU in the abdominal skin. Mortality was followed for 14 days. To study bacterial spread and host responses, groups of 5 mice were killed on days 1–4 after infection, and their blood, spleen, liver (1 lobe), lungs, inguinal lymph nodes, and femurs were collected. Half of the spleen and liver was fixed for immunohistological analyses, and the other half, the lungs, and the inguinal lymph nodes were homogenized using glass beads (VWR) to evaluate bacterial load. The remaining supernatants of grinded organs and serum were sterile filtered and frozen for cytokine measurement. Blood formula was determined using a Vet ABC counter (SCIL).

### Immunohistological Analyses

Organs fixed with 4% paraformaldehyde were dehydrated and embedded in paraffin. Five-micrometer sections were stained with hematoxylin-eosin. Polymorphonuclear neutrophils (PMNs) were quantified microscopically using a score ranging from 0 (normal) to 5 (large areas filled with infiltrating PMNs), and hemorrhages were scored from 0 (normal) to 3 (extended hemorrhages) on ≥3 complete sections per sample. For immunohistological labeling of bacteria, sections were incubated with a *Y. pestis* F1-specific rabbit antiserum (Institut Pasteur) followed by rabbit-specific Histofine MAX-PO (Nichirei). Peroxidase was detected using the AminoEthyl Carbazole (AEC) substrate (Sigma) with hematoxylin counterstaining.

### Cytokine/Chemokine Assays

Measurement of IL-1α, IL-1β, IL-10, tumor necrosis factor (TNF)–α, interferon (IFN) γ, IL-6, IL-12p70, granulocyte colony-stimulating factor (G-CSF), keratinocyte-derived chemokine (KC/CXCL1), and macrophage cationic peptide-1 (MCP-1) was performed with the BioPlex cytokine bead array (Bio-Rad) using a Luminex platform.

### Flow Cytometry Analyses

Minced bone marrow and spleen tissues were passed through a 70-μm mesh (BD biosciences), and red cells were lysed using Gey's method [20]. Polymorphonuclear neutrophils ($CD11b^+Ly6G^{hi}SSC^{hi}$), T cells ($TCR^+$), bone marrow monocytes ($CD11b^+Ly6G\text{-}SSC^{int}$), spleen red pulp macrophages ($F4/80^+CD11b^-Ly6G^-$), and other macrophages ($CD11b^+F4/80^-Ly6G^-$) were quantified using specific fluorescent antibodies: anti-CD11b–Pacific Blue (eBiosciences), anti-TCR-β–Alexa 488, anti-F4/80–allophycocyanin (Invitrogen), and anti-Ly6G–phycoerythrin monoclonal antibody clone 1A8 (BD Biosciences). Cells were analyzed with a CyAn cytometer (Beckman-Coulter).

### Statistical Analyses

Statistical analyses included the Mann–Whitney–Wilcoxon test (quantitative parameters), Spearman test (CFU and cytokine contents), and Fisher exact test (mortality).

## RESULTS

### Mouse Infections

To compare the progression of the infection and the host response in susceptible and resistant mice, 29 SEG and 30 B6 animals were infected subcutaneously with 100 CFU of *Y. pestis* CO92. A group of 9 or 10 animals was kept to follow mortality for 14 days (mortality group), and the 20 remaining mice (study group) were distributed in 4 cages to be analyzed on days 1–4 after infection. Ascribing the day of death a priori to each group prevented the bias of selecting in the latest days the animals that resisted infection better in the early phase.

In the mortality group, B6 mice started to develop clinical symptoms of infection and to die on day 3 after infection, and 18 of 20 were dead on day 14. In contrast, SEG mice developed clinical signs of disease, such as prostration and ruffled fur earlier (day 2) but started to recover on day 4, and 17 of 19 animals survived and looked healthy on day 14. The difference in survival was highly significant ($P < .0001$). Body weight variations correlated with symptoms. Body weight loss in B6 mice began on day 3 and reached 10% on day 4, while body weight of SEG mice remained constant (Supplementary figure 1*A*). In the study group, 1 B6 mouse died on day, and therefore only 9 animals were available for study at this time point.

### Comparison of the Infectious Process in SEG and B6 Mice

Bacterial loads in SEG and B6 mice followed clearly distinct kinetics over the 4-day study period. A few circulating *Y. pestis* cells were detected in the blood of both mouse strains on day 1, but they reached much higher numbers in the blood of SEG mice on day 2 (Figure 1*A*). However, bacteremia subsequently decreased in SEG mice while it increased in B6 mice, so that similar CFU values were found on day 3 in the blood of the 2 mouse strains. On day 4, SEG mice had cleared circulating bacteria while the bacterial load had continued to rise in B6 mice.

Remarkably, a similar higher bacterial load was observed in all collected organs of SEG mice (although the difference was statistically significant only in the lungs) on day 2 (Figure 1*B–E*). The bacterial loads then stabilized and started to decline in most SEG organs. In contrast *Y. pestis* numbers rose continuously in B6 tissues, so that much higher bacterial loads were found in all B6 tissues analyzed (except lungs) on day 4. The kinetics of infection was highly reproducible for the 2 groups of mice during 2 independent experiments. Therefore, both susceptible and resistant mice were efficiently colonized by *Y. pestis*, but SEG mice displayed an earlier bacterial invasion that was transient.

### *Y. pestis* Growth in Serum of SEG and B6 Mice

Since one of the most remarkable differences between resistant and susceptible animals was the capacity of SEG mice to clear circulating bacteria, we questioned whether a bactericidal component with a higher activity or concentration could be present at homeostasis or produced during infection in the serum of resistant mice. The growth curves of *Y. pestis* were similar in the undecomplemented serum samples of the 2 mouse strains before and 2 days after infection (Supplementary figure 1*B*), indicating that SEG resistance is not attributable to the presence or release of a circulating antibacterial compound.

### SEG and B6 Blood Cell Populations During the Infectious Process

Because bacterial clearance from the blood stream may also result from a cell-mediated process, the circulating cell populations during the course of infection were analyzed in SEG and B6 mice. A significant increase in blood leukocyte numbers was observed between day 0 and day 1 in both mouse strains ($P < .02$). However, leukocytosis persisted in SEG mice but not in B6 mice, so that a marked difference in blood leukocytes was observed on day 4 (Figure 2*Aa*). The same trend was noted for platelets (Figure 2*Ab*), but erythrocyte counts remained stable (Figure 2*Ac*), showing the specific increase of some blood cell populations in SEG mice. Within the leukocyte populations, lymphocyte, monocyte, and PMN cell counts rose in the 2 mouse strains on days 1 and 2 after infection (Figure 2*Ad–f*). Counts for PMNs and monocytes (but not lymphocytes) continued to increase over the study period, moderately in B6 mice and much more significantly in SEG mice.

Because the marked difference in circulating PMNs and monocytes on day 4 could result from a more efficient hematopoiesis in SEG mice, we examined the bone marrow cell populations in the 2 mouse strains. Before infection, the total cell content in the femurs was significantly higher ($P = .0008$) in B6 mice ($31 \pm 0.4 \times 10^6$) than in SEG mice ($21 \pm 1.9 \times 10^6$), probably because of the larger body size of B6 mice ($19.8 \pm 0.6$ g) compared with SEG mice ($16.6 \pm 1.6$ g). The percentages of PMNs and monocytes in the bone marrow were nonetheless similar in the 2 species but became significantly higher in SEG mice on day 4 (Figure 2*B*), suggesting a more efficient bone marrow hematopoiesis at a late stage of infection in resistant mice.

### Tissue Lesions in Infected B6 and SEG Mice

The liver of the 2 mouse strains exhibited similar histological lesions (mild inflammation with occasional weak hemorrhages and PMN infiltrates), which were moderate at all time points (data not shown). In contrast, tissue lesions characterized by a mild inflammatory infiltrate primarily composed of PMNs were observed in the spleen of B6 and SEG mice on days 1 and 2 and subsequently became more pronounced in B6 mice (Figure 3*A*). Hemorrhages appearing on day 2 and

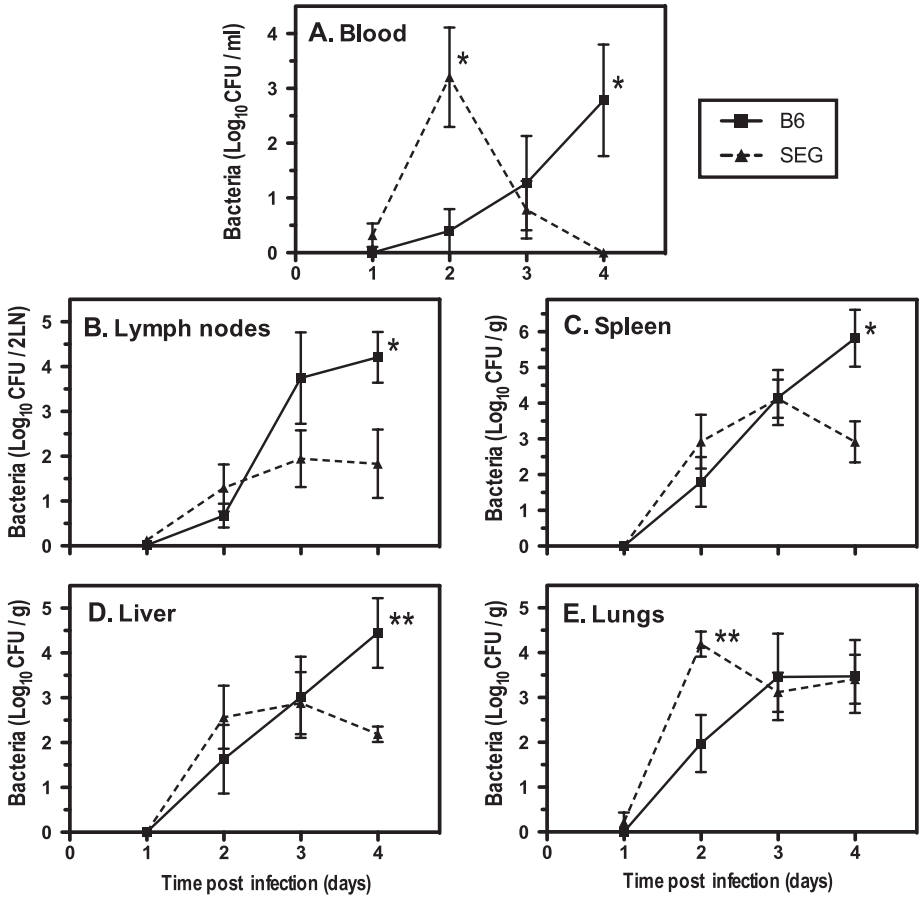


**Figure 1.** Bacterial loads at different time points in the blood and organs of *Yersinia pestis*–infected B6 and SEG mice. Mice were infected subcutaneously with 100 colony-forming units (CFU) of CO92, and groups of 10 animals (combined results of 2 independent experiments) were killed on days 1–4 after infection. The bacterial loads in the blood, lymph nodes (LN), spleen, liver, and lung were determined for each animal and at each time point. Data shown are means ± standard errors of the mean for 9 or 10 mice per point. Differences between the 2 mouse strains at each time point were evaluated statistically using the Mann–Whitney–Wilcoxon rank sum test. $^{*}P < .05$; $^{**}P < .01$.

increasing over time were always more extended in the spleens of B6 mice. At late time points (day 4), the spleens of B6 mice exhibited necrotic lesions destroying the red pulp (Figure 3*Ba*) and containing free bacteria (Figure 3*Bc*). In contrast, microabscesses appearing as rare and well-contained round foci of PMN infiltration without necrosis started to develop on day 4 in the spleens of SEG mice (Figure 3*Bb*), and bacteria were mostly found within these microabscesses (Figure 3*Bd*). The infectious course in SEG mice thus differs from that in B6 mice and is characterized by less destructive lesions of the spleen and the capacity to circumscribe bacterial foci.

### Spleen Cell Populations in Uninfected or Infected B6 and SEG Mice

To further investigate the differences in spleen responses, groups of 6 or 7 B6 and SEG mice were killed before infection or on day 2 after infection, and their spleen cell populations were analyzed. The experiments were done twice and the results were pooled. In noninfected animals, total spleen cells were higher in number in B6, as expected from their larger spleen size (31 ± 18 mg in B6 vs 16 ± 4 mg in SEG). Both mouse strains had similar proportions of F4/80 ± $CD11b^{+}$ macrophages and undetectable PMN ($CD11b^{+}Ly6G^{+}$) levels (Figure 3*C*, diamonds). The main difference was a higher percentage of T cells in B6 mice and of $F4/80^{+}CD11b^{-}$ macrophages in SEG mice.

After 2 days of infection, total splenocytes increased in the 2 mouse groups, indicating an early cell recruitment (Figure 3*C*, circles). The drop in T-lymphocyte percentages in both mouse groups demonstrated that this cell enrichment was not due to an adaptive response. The proportion of $CD11b^{+}$ macrophages was not significantly affected by the infection. In agreement with our histological observations, the moderate recruitment of PMNs (≈1.5% of spleen cells) observed in the 2 mouse strains could not account for the increased spleen cellularity on day 2. The major change in both infected mouse strains was a significant increase in the $F4/80^{+}CD11b^{-}$ macrophage population, which was considerably higher in SEG mice. Actually, this cell type represented 40% of the splenocytes in infected spleens of SEG

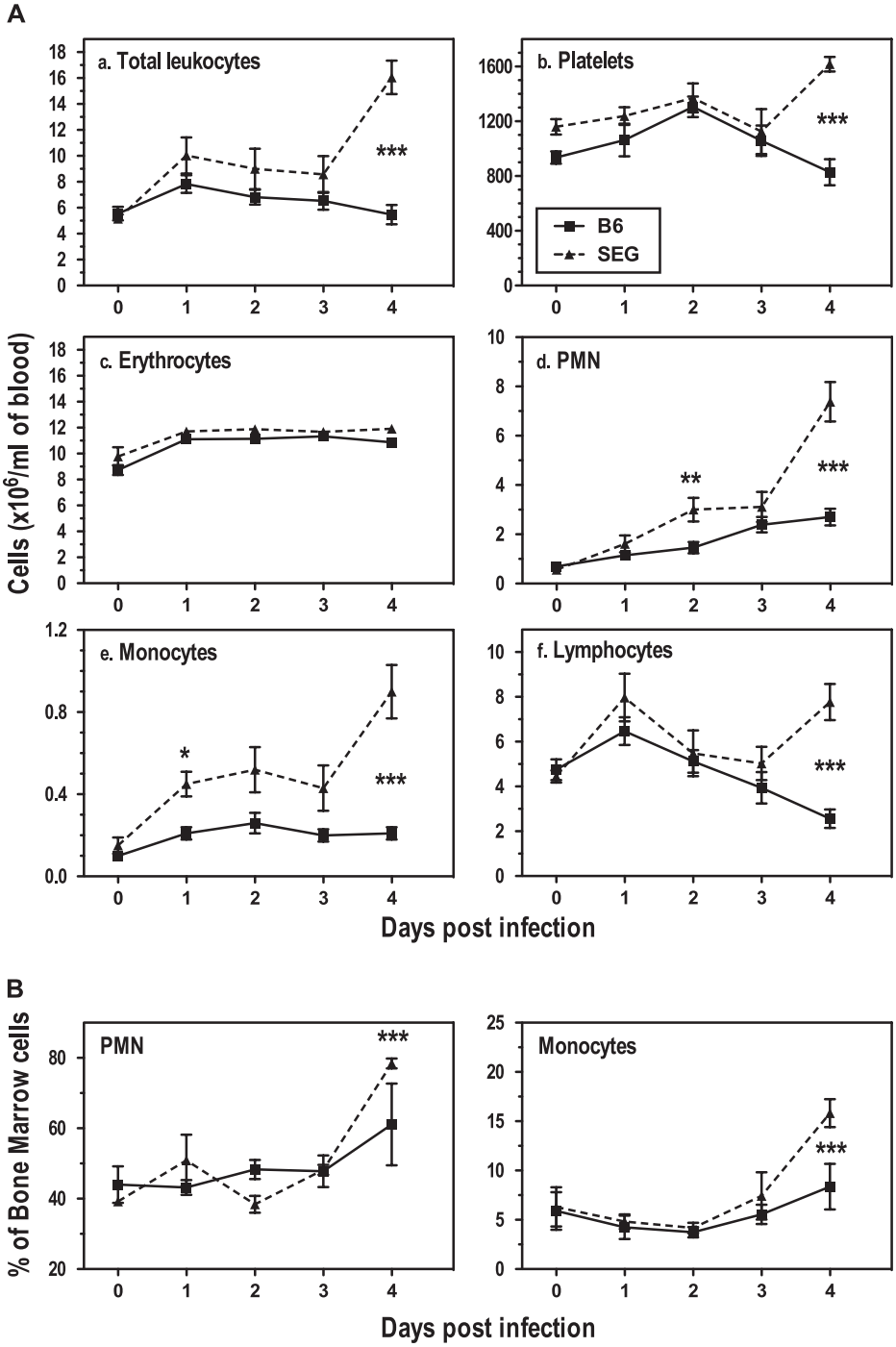


**Figure 2.** Blood (*A*) and bone marrow (*B*) cell numbers during the course of infection in SEG and B6 mice. Data shown are means ± standard errors of the mean for 9 or 10 mice (blood) or 5 mice (bone marrow) at each time point. Differences between the 2 mouse strains at each time point were evaluated statistically using the Mann–Whitney–Wilcoxon rank sum test. Abbreviation: PMN, polymorphonuclear neutrophil. $^{*}P < .05$; $^{**}P < .01$; $^{***}P < .001$.

mice versus ≈15% in the spleens of B6 mice. Immunohistolabeling of the F4/80 antigen in spleen sections indicated that all F4/80$^{+}$ macrophages were located in the red pulp (data not shown). Therefore, SEG mice have a higher basal level of F4/80$^{+}$ red pulp macrophages and they show a remarkable expansion during infection.

### Kinetics of Cytokine Release in the Blood and Organs of SEG and B6 Mice

The production of 10 cytokines known to participate to the innate immune response was quantified in the plasma, lymph nodes, and spleen of SEG and B6 mice during the course of infection. Five cytokines (IFN-γ, TNF-α, IL-1β, IL-10, and IL-12p70)

A

| | Day 1 | | Day 2 | | Day 3 | | Day 4 | |
|---|---|---|---|---|---|---|---|---|
| | B6 | SEG | B6 | SEG | B6 | SEG | B6 | SEG |
| **Mean score** | | | | | | | | |
| Hemorrhages | 0 | 0 | 0.6 (±0.1) * | 0.2 (±0.1) | 1.0 (±0.1) ** | 0.3 (±0.1) | 1.0 (±0.2) | 0.4 (±0.2) |
| PMN infiltrates | 0.3 (±0.1) | 0.3 (±0.1) | 0.6 (±0.1) | 0.5 (±0.1) | 1.3 (±0.2) * | 0.9 (±0.1) | 1.9 (±0.5) | 1.3 (±0.2) |
| **No of mice affected/total** | | | | | | | | |
| Congestion | 1/10 | 1/10 | 0/10 | 0/10 | 2/10 | 4/10 | 3/9 | 2/10 |
| Necrosis | 0/10 | 0/10 | 0/10 | 0/10 | 0/10 | 0/10 | 3/9 | 0/10 |
| Micro abscesses | 0/10 | 0/10 | 0/10 | 0/10 | 1/10 | 1/10 | 0/9 | 3/10 |

B

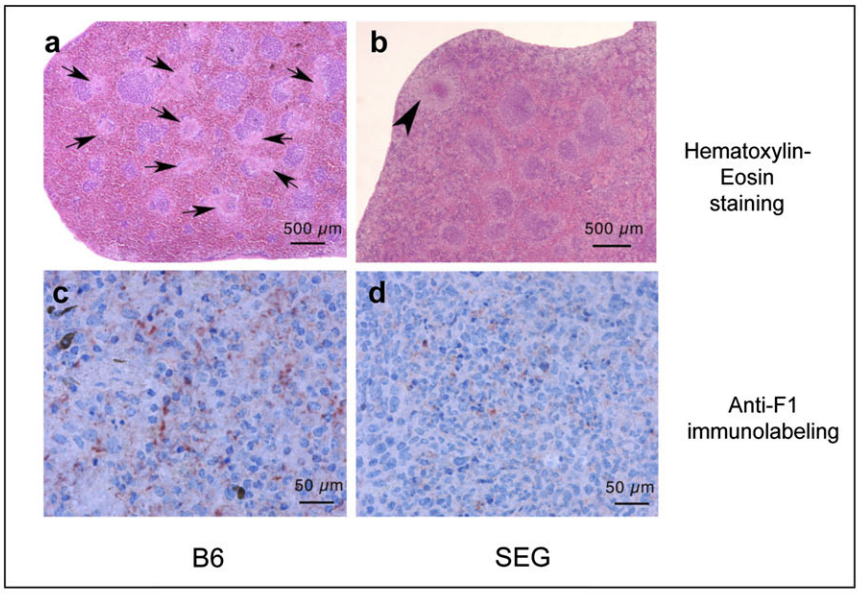


C

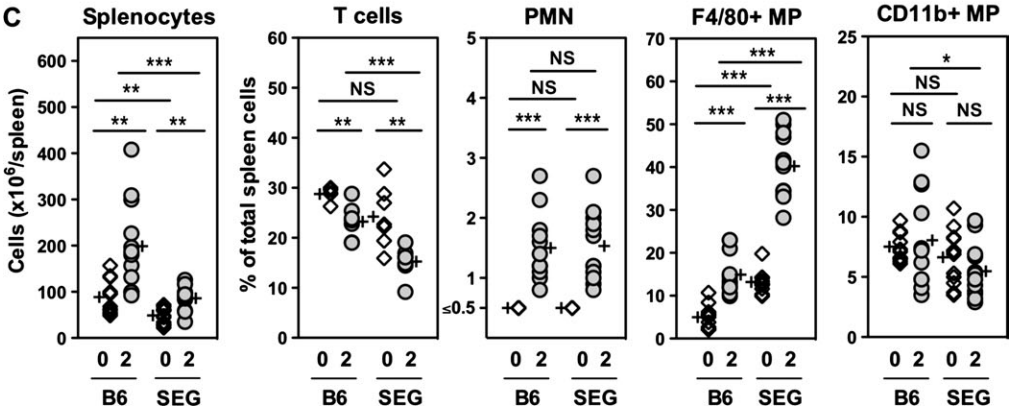


**Figure 3.** Tissue lesions and cell populations in the spleens of infected SEG and B6 mice. *A*, Histological lesions in the spleen: Scores (means ± standard errors of the mean) of hemorrhages (histological scale, 0 to 3) and polymorphonuclear neutrophil (PMN) infiltration (scale, 0–5) summarize the observation of ≥60 microscopic fields (≥20 fields/section with a ×20 objective on ≥3 complete sections per sample). Mice (positive / total) were considered as positive when the indicated lesions had a score ≥1.5/5. *B*, Hematoxylin-eosin (*a*, *b*) and anti-F1 immunohistochemical staining (*c*, *d*) of spleen sections obtained on day 4 after infection. The spleens of B6 mice had abundant foci of necrosis (*arrows in a*) containing numerous bacteria (*red-brown color in c*), whereas the spleens of SEG mice exhibited some microabscesses (*arrowhead in b*) without necrosis and containing few bacteria (*d*). Two-tailed nonparametric Mann–Whitney–Wilcoxon rank sum test was used to compare groups. $*P \leq .05$; $**P \leq .01$. *C*, Quantification of different spleen cell populations in B6 and SEG mice (12 animals each from 2 independent experiments, except for T cells, for which 7 animals were analyzed). Splenocytes were counted microscopically and macrophages (MP), polymorphonuclear neutrophils (PMN), and T cells were quantified by flow cytometry. Individual results from uninfected (day 0, white diamonds) or infected (day 2 after infection, gray circles) animals are plotted. Plus signs indicate mean values. Two-tailed nonparametric Mann–Whitney–Wilcoxon rank sum test was used to compare groups. $*P \leq .05$; $**P \leq .01$; $***P \leq .001$. Abbreviation: NS, not significant.

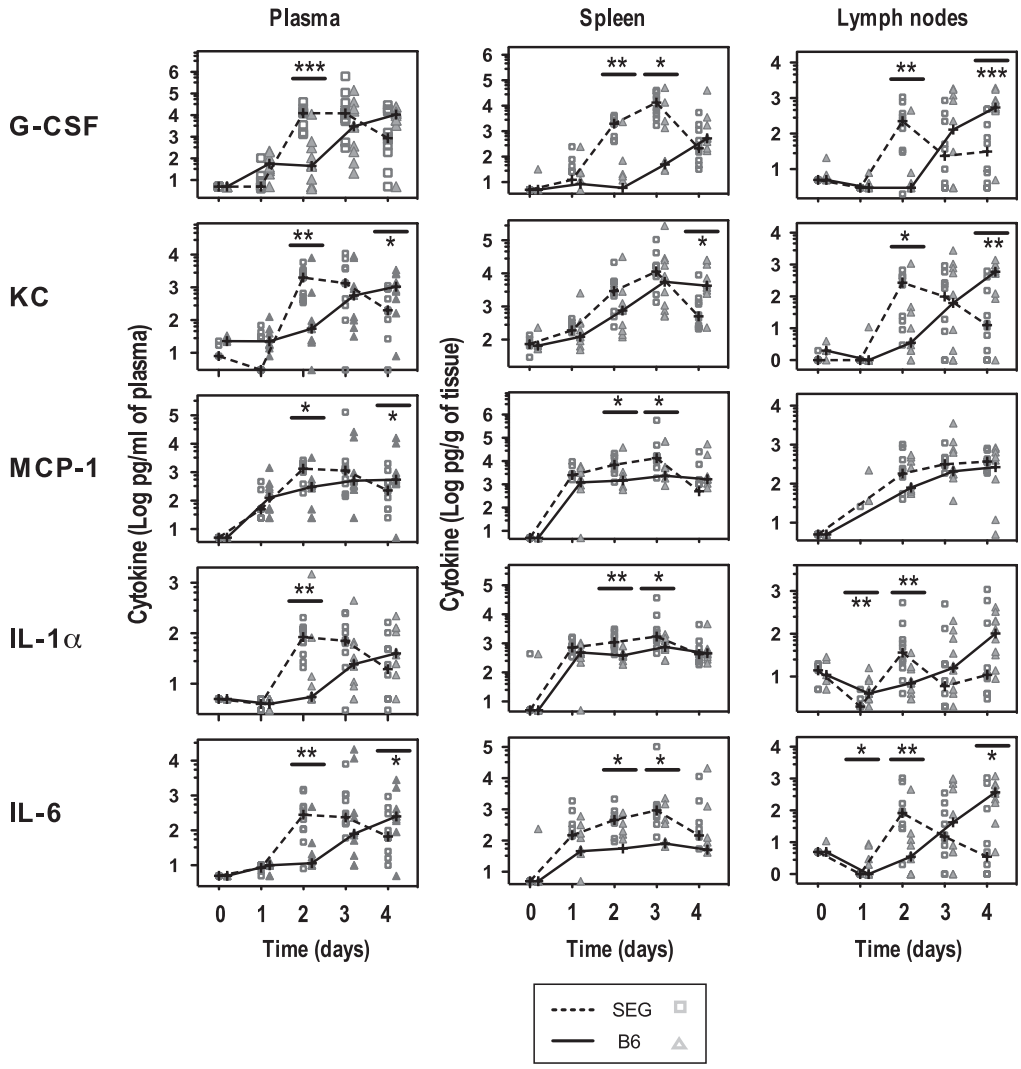


**Figure 4.** Cytokine contents in the plasma, spleen, and inguinal lymph nodes of B6 and SEG mice during the course of a *Yersinia pestis* infection. Data shown are the values for 5 cytokines (granulocyte colony-stimulating factor [G-CSF], keratinocyte-derived chemokine [KC], macrophage cationic peptide-1 [MCP-1], interleukin [IL]–1α and IL-6) in individual SEG (rectangles) and B6 (triangles) mice from day 0 to day 4 after infection for 10 animals (9 for B6 on day 4) and the median curves (solid lines for B6 mice, dotted lines for SEG mice). Groups were compared using the nonparametric Mann–Whitney–Wilcoxon rank sum test. Asterisks above comparison bar indicate values significantly superior in SEG mice; asterisks below comparison bar, values significantly superior in B6 mice. *$P \leq .05$; **$P \leq .01$; ***$P \leq .001$.

exhibited similar levels of production in the 2 mouse strains during the infectious process, despite higher levels of 4 of them in the plasma of B6 mice before infection (Supplementary figure 2).

The other 5 cytokines (G-CSF, keratinocyte-derived chemokine [KC], macrophage cationic peptide-1 [MCP-1], IL-1α, and IL-6) displayed clear differences in the kinetics of production between the 2 mouse strains (Figure 4). Most remarkably, their levels were correlated in the 3 biological samples tested. The pattern in SEG was characterized by a peak of production in the plasma and lymph nodes on day 2 and in the spleen on day 3. The levels of these cytokines were significantly lower in the organs of B6 mice at the same time points. At a later stage of infection (day 4), the amounts of these 5 cytokines started to decline in SEG organs, while they continued to rise or remained high (MCP-1) in B6 organs, so that higher levels were detected in the plasma and lymph nodes of B6 mice on day 4. Therefore, *Y. pestis* infection in resistant mice was characterized by a faster but transient production of G-CSF, KC, MCP-1, IL-1α, and IL-6, whereas susceptible mice displayed a delayed but continuously increasing cytokine response.

### Correlation Between Cytokine Release and Bacterial Load in SEG and B6 Mice

Interestingly, the kinetics of production of these 5 cytokines in SEG and B6 mice seemed to parallel the bacterial loads observed in the 2 mouse strains. Because CFU and cytokine data were

**Table 1. Correlation Between Bacterial Load and Cytokine Content in Tissues of Infected Mice**

| | SEG Mice | | | B6 Mice | | |
|---|---|---|---|---|---|---|
| Cytokine | Plasma | Spleen | Lymph Nodes | Plasma | Spleen | Lymph Nodes |
| G-CSF | | | | | | |
| *r* | 0.50 | 0.67 | 0.45 | 0.69 | 0.68 | 0.57 |
| *P* | .0005 | <.0001 | .002 | <.0001 | <.0001 | <.0001 |
| IL-1α | | | | | | |
| *r* | 0.41 | 0.57 | 0.39 | 0.57 | 0.55 | 0.50 |
| *P* | .005 | <.0001 | .009 | <.0001 | .0001 | .0005 |
| IL-6 | | | | | | |
| *r* | 0.52 | 0.54 | 0.32 | 0.70 | 0.39 | 0.54 |
| *P* | .0002 | .0001 | NSS | <.0001 | NSS | .0001 |
| KC | | | | | | |
| *r* | 0.51 | 0.75 | 0.57 | 0.59 | 0.84 | 0.64 |
| *P* | .0003 | <.0001 | <.0001 | <.0001 | <.0001 | <.0001 |
| MCP-1 | | | | | | |
| *r* | 0.62 | 0.54 | 0.23 | 0.71 | 0.42 | 0.45 |
| *P* | <.0001 | .0001 | NSS | <.0001 | .005 | .002 |
| IL-1β | | | | | | |
| *r* | 0.27 | 0.57 | 0.22 | 0.23 | 0.52 | 0.44 |
| *P* | NSS | <.0001 | NSS | NSS | .0003 | .003 |
| IL-10 | | | | | | |
| *r* | 0.12 | −0.19 | −0.37 | −0.26 | −0.11 | −0.19 |
| *P* | NSS | NSS | NSS | NSS | NSS | NSS |
| TNF-α | | | | | | |
| *r* | 0.41 | 0.17 | −0.10 | 0.54 | 0.18 | 0.05 |
| *P* | .005 | NSS | NSS | .0002 | NSS | NSS |
| IFN-γ | | | | | | |
| *r* | 0.23 | 0.20 | −0.07 | 0.19 | 0.14 | 0.06 |
| *P* | NSS | NSS | NSS | NSS | NSS | NSS |
| IL-12p70 | | | | | | |
| *r* | 0.53 | 0.15 | 0.08 | 0.43 | 0.19 | −0.01 |
| *P* | .0002 | NSS | NSS | NSS | NSS | NSS |

The nonparametric Spearman rank test (*r*) was used to evaluate the correlation between colony-forming unit values and the level of each cytokine, regardless of the time after infection. To account for multiple testing, a Bonferroni correction was applied, so only correlation values with *P* values <.01 were considered as statistically significant; in such cases, only *r* values are given. For SEG mice, 40 samples were tested; for B6 mice, 39 samples, in all sites.

Abbreviations: G-CSF, granulocyte colony-stimulating factor; IL, interleukin; IFN, interferon; KC, keratinocyte-derived chemokine; MCP-1, macrophage cationic peptide-1; NSS, not statistically significant; TNF, tumor necrosis factor.

available for each individual animal, the association between the bacterial burden in the plasma, spleen, and lymph nodes (whatever the infection day) and the release of the 10 cytokines studied was investigated. The levels of the 5 cytokines that were not produced differently in B6 versus SEG mice (IFN-γ, TNF-α, IL-1β, IL-10, and IL-12p70) were most often not correlated with bacterial loads (Table1). In contrast, a remarkable and significant correlation was observed between the levels of G-CSF, KC, MCP-1, IL-1α, and IL-6 and the number of bacteria present in most mouse organs (Table 1). This correlation was true for both SEG and B6 mice. Our results thus indicate that even if the kinetics of production of these 5 cytokines differed between susceptible and resistant mice, both mouse strains have the capacity to develop the same cytokine response when exposed to similar bacterial loads.

## DISCUSSION

The wild-derived SEG mouse strain naturally exhibits an exceptional capacity to resist an otherwise lethal subcutaneous infection with *Y. pestis* [18]. We took advantage of this unprecedented ability to survive bubonic plague to study pathophysiological mechanisms and host responses associated with the resistance phenotype. To do so, the course of infection and innate immune response were compared in resistant SEG and susceptible B6 mouse strains. The most remarkable and unexpected feature

that emerged from this comparison was that *Y. pestis* colonized the organs of resistant mice rapidly and more efficiently. This was evidenced by clinical symptoms of infection that appeared on day in SEG mice, and were retarded (day 4) in B6 mice.

The higher bacterial load in SEG mice on day 2 was accompanied by a higher in situ production of 5 cytokines (G-CSF, KC, MCP-1, IL-1α, and IL-6). This rapid cytokine release is most likely the direct consequence of the bacterial burden, because we found a highly significant correlation between the CFU value and cytokine levels in each organ of each individual mouse tested. Of note, this correlation was not observed for the other 5 cytokines analyzed (IFN-γ, TNF-α, IL-1β, IL-10, and IL-12p70). A characteristic of the former group is that, in addition to being produced by bone marrow derived cells, they all are also released by somatic cells, such as endothelial cells, fibroblasts, and keratinocytes. This points at stromal cells rather than immune cells as a potential source for the early and coordinate production of G-CSF, KC, MCP-1, IL-1α, and IL-6 on stimulation by *Y. pestis*.

This early release may explain the higher numbers of circulating blood monocytes and PMN in SEG mice on day 2. Indeed, MCP-1 is one of the key chemokines that regulate migration and infiltration of monocytes and macrophages at inflammatory sites [21, 22]. Granulocyte colony-stimulating factor and IL-6 induce granulocyte mobilization from the bone marrow and their activation, differentiation, and survival [23–25], and KC and IL-1α promote their chemotaxis [26, 27]. Because neutrophils and monocytes are key components of the host innate response to many bacterial pathogens [28–30], they most likely participate actively in *Y. pestis* clearance from the blood of SEG mice.

The early time points of infection in SEG mice were also characterized by a massive and specific expansion of $F4/80^+CD11b^-$ macrophages in the spleen, an organ important for capturing circulating bacteria. $F4/80^+CD11b^-$ macrophages reside in the liver (Kupffer cells) and the spleen, in which they are restricted to the red pulp. Therefore, in contrast to $CD11b^+$ macrophages, they are not in contact with lymphocytes and thus are not key players in the adaptive immunity. They are rather effectors of the innate response by phagocytosing blood bacteria penetrating into the highly vascularized red pulp of the spleen and by producing microbicidal metabolites [31]. $F4/80^+CD11b^-$ macrophages may thus be critical for the ability of SEG mice to respond rapidly and efficiently to a *Y. pestis* infection. An afflux of spleen macrophages was not observed in resistant 129 mice [17], indicating a distinct innate response in these mice. It is worth noting that the proportion of this subpopulation was already higher in SEG mice than B6 mice before infection, suggesting that SEG mice are already ''preprogrammed'' to mount a more efficient $F4/80^+CD11b^-$–mediated cellular response.

Day 2 appears as a critical time point at which the host response is already committed to resistance or susceptibility. The differences observed later during infection (days 3 and 4) may therefore simply reflect the consequences of an engagement of the host response toward bacterial clearance or multiplication. Indeed, later time points showed the containment and progressive decrease in the bacterial load in SEG mice (with a complete recovery of most animals) and a continuous increase in the bacterial burden in B6 mice, followed by their death. The more abundant hematopoiesis and circulating blood cells observed in SEG mice on day 4, as well as their capacity to trap spleen bacteria within a cellular reaction preventing massive destructive lesions, may thus reflect the results of the early triggering of an efficient innate immune response in resistant animals, rather than being the cause of their recovery. Another argument that the earliness of the response is crucial for resistance is our observation that the 2 mouse strains had the capacity to elicit the same effective G-CSF, KC, MCP-1, IL-1α, and IL-6 responses when exposed to comparable bacterial loads. This would be supported by the fact that, except for the *il6R* gene, no genetic determinant corresponding to these 5 cytokines is located on the 3 mouse chromosomal loci recently shown by us to be associated with SEG resistance to plague [18]. Thus, the major difference between B6 and SEG mice is not the quality of their cytokine responses but the time when they are triggered. In conclusion, comparison of the *Y. pestis* infection course and innate immune response in susceptible and resistant mouse strains has shown that, unexpectedly, the more efficient colonization of SEG mice by *Y. pestis* early during the infectious process may be critical for the triggering of an effective innate immune response.

## Supplementary Data

Supplementary materials are available at *The Journal of Infectious Diseases* online (http://www.oxfordjournals.org/our_journals/jid/). Supplementary materials consist of data provided by the author that are published to benefit the reader. The posted materials are not copyedited. The contents of all supplementary data are the sole responsibility of the authors. Questions or messages regarding errors should be addressed to the author.

## Notes

***Acknowledgments.*** The authors wish to thank Professor J. L. Guénet for his support of the project and A. Ferreira for help with flow cytometry.

***Financial support.*** This work was supported by the French Ministry of Health (BIOTOX multi-organism grant) funded by Aventis Pharma (Sanofi-Aventis group) and Bayer Pharma. C. B. is a recipient of a Délégation Générale pour l'Armement fellowship. The Mouse Functional Genetics Unit is supported by Merck Serono.

***Potential conflict of interest.*** All authors: No reported conflicts.

All authors have submitted the ICMJE Form for Disclosure of Potential Conflicts of Interest. Conflicts that the editors consider relevant to the content of the manuscript have been disclosed.

## References

1. Perry RD, Fetherston JD. *Yersinia pestis*—etiologic agent of plague. Clin Microbiol Rev **1997**; 10:35–66.
2. Inglesby TV, Dennis DT, Henderson DA, et al. Plague as a biological weapon—medical and public health management. J Am Med Assoc **2000**; 283:2281–90.

3. World Health Organization. Human plague in 2002 and 2003. Wkly Epidemiol Rec **2004**; 79:301–8.
4. World Health Organization. International meeting on preventing and controlling plague: the old calamity still has a future. Wkly Epidemiol Rec **2006**; 81:278–84.
5. Guiyoule A, Gerbaud G, Buchrieser C, et al. Transferable plasmid-mediated resistance to streptomycin in a clinical isolate of *Yersinia pestis*. Emerg Infect Dis **2001**; 7:43–8.
6. Galimand M, Guiyoule A, Gerbaud G, et al. Multidrug resistance in *Yersinia pestis* mediated by a transferable plasmid. N Engl J Med **1997**; 337:677–80.
7. Guinet F, Ave P, Jones L, Huerre M, Carniel E. Defective innate cell response and lymph node infiltration specify *Yersinia pestis* infection. PLoS One **2008**; 3:e1688.
8. Sebbane F, Gardner D, Long D, Gowen BB, Hinnebusch BJ. Kinetics of disease progression and host response in a rat model of bubonic plague. Am J Pathol **2005**; 166:1427–39.
9. Thomas RE, Barnes AM, Quan TJ, Beard ML, Carter LG, Hopla CE. Susceptibility to *Yersinia pestis* in the northern grasshopper mouse (*Onychomys leucogaster*). J Wildl Dis **1988**; 24:327–33.
10. Rahalison L, Ranjalahy M, Duplantier JM, et al. Susceptibility to plague of the rodents in Antananarivo, Madagascar: the genus Yersinia. Vol 529. New York: Kluwer Academis/Plenum Publishers, **2003**; 439–42.
11. Quan SF, Kartman L. Ecological studies of wild rodent plague in the San Francisco Bay area of California. VIII. Susceptibilité of wild rodents to experimental plague infection. Zoonoses Res **1962**; 1:121–44.
12. Hubbert WT, Goldenberg MI. Natural resistance to plague: genetic basis in the vole (*Microtus californicus*). Am J Trop Med Hyg **1970**; 19:1015–9.
13. Russel P, Eley SM, Hibbs SE, Manchee RJ, Stagg AJ, Titball RW. A comparison of plague vaccine, USP and EV76 vaccine induced protection against *Yersinia pestis* in a murine model. Vaccine **1995**; 13:1551–6.
14. Philipovskiy AV, Cowan C, Wulff-Strobel CR, et al. Antibody against V antigen prevents Yop-dependent growth of *Yersinia pestis*. Infect Immun **2005**; 73:1532–42.
15. Turner JK, McAllister MM, Xu JL, Tapping RI. The resistance of BALB/cJ mice to *Yersinia pestis* maps to the major histocompatibility complex of chromosome 17. Infect Immun **2008**; 76:4092–9.
16. Turner JK, Xu JL, Tapping RI. Substrains of 129 mice are resistant to *Yersinia pestis* KIM5: implications for interleukin-10–deficient mice. Infect Immun **2009**; 77:367–73.
17. Congleton YH, Wulff CR, Kerschen EJ, Straley SC. Mice naturally resistant to *Yersinia pestis* delta pgm strains commonly used in pathogenicity studies. Infect Immun **2006**; 74:6501–4.
18. Blanchet C, Jaubert J, Carniel E, et al. Mus spretus SEG/Pas mice resist virulent *Yersinia pestis*, under multigenic control. Genes Immun **2011**; 12:23–30.
19. Guenet JL, Bonhomme F. Wild mice: an ever-increasing contribution to a popular mammalian model. Trends Genet **2003**; 19:24–31.
20. Mishell B, Shiigi S. Selected methods in cellular immunology. San Francisco: WH Freeman, **1980**.
21. Serbina NV, Pamer EG. Monocyte emigration from bone marrow during bacterial infection requires signals mediated by chemokine receptor CCR2. Nat Immunol **2006**; 7:311–7.
22. Deshmane SL, Kremlev S, Amini S, Sawaya BE. Monocyte chemoattractant protein-1 (MCP-1): an overview. J Interferon Cytokine Res **2009**; 29:313–26.
23. Semerad CL, Liu F, Gregory AD, Stumpf K, Link DC. G-CSF is an essential regulator of neutrophil trafficking from the bone marrow to the blood. Immunity **2002**; 17:413–23.
24. Walker F, Zhang HH, Matthews V, et al. IL6/sIL6R complex contributes to emergency granulopoietic responses in G-CSF– and GM-CSF–deficient mice. Blood **2008**; 111:3978–85.
25. Maianski NA, Mul FP, van Buul JD, Roos D, Kuijpers TW. Granulocyte colony-stimulating factor inhibits the mitochondria-dependent activation of caspase-3 in neutrophils. Blood **2002**; 99:672–9.
26. Ozaki Y, Ohashi T, Kume S. Potentiation of neutrophil function by recombinant DNA–produced interleukin 1a. J Leukoc Biol **1987**; 42:621–7.
27. Lira SA, Zalamea P, Heinrich JN, et al. Expression of the chemokine N51/KC in the thymus and epidermis of transgenic mice results in marked infiltration of a single class of inflammatory cells. J Exp Med **1994**; 180:2039–48.
28. Segal AW. How neutrophils kill microbes. Annu Rev Immunol **2005**; 23:197–223.
29. Serbina NV, Salazar-Mather TP, Biron CA, Kuziel WA, Pamer EG. TNF/iNOS-producing dendritic cells mediate innate immune defense against bacterial infection. Immunity **2003**; 19:59–70.
30. Goodyear A, Jones A, Troyer R, Bielefeldt-Ohmann H, Dow S. Critical protective role for MCP-1 in pneumonic *Burkholderia mallei* infection. J Immunol **2009**; 184:1445–54.
31. Adams DO, Hamilton TA. The cell biology of macrophage activation. Annu Rev Immunol **1984**; 2:283–318.